DESIGN STUDIES ON AN EXTERNAL ROTOR PERMANENT MAGNET SYNCHRONOUS MACHINE FOR A POSITION SENSORLESS CONTROL — COMPARISON OF Y- AND Δ-CONNECTED STATOR WINDING

Erich Schmidt, *Member, IEEE*, Marko Sušić
Institute of Electrical Drives and Machines, Vienna University of Technology, Vienna, Austria
erich.schmidt@ieam.tuwien.ac.at

Abstract – The permanent magnet synchronous machine with an external rotor is the most important device for high performance electrical drive systems in particular for hybrid electric vehicles. With such an application, the machine will operate in a wide speed range and on the other hand with very fast changing loads in both motor and generator operational modes. The paper discusses finite element analyses for the optimization of a permanent magnet machine with an external rotor in terms of a comparison of a Y- and Δ-connected stator winding and the influence on the electromagnetic torque as one of the most important design parameter.

Keywords – Permanent magnet machine, Position sensorless control, Finite element analysis

1. INTRODUCTION

The permanent magnet excited synchronous machine (PMSM) with an external rotor gains in importance particularly with the automotive industry turn-over to highly efficient machines utilized for hybrid drive solutions. For such an application, there are two keypoints for the machine design [1], [2]. First, the torque ripple shows high significance and should be as small as possible. Secondly, a position sensorless control scheme necessary for a robust drive design requires a magnetic saliency even with fast changing load conditions.

Regarding the first mentioned keypoint, the paper discusses parametric finite element analyses of a PMSM with an external rotor. With the intent of an optimized design in terms of cogging torque and magnetic saliency, current driven analyses of various stator designs are carried out to obtain the electromagnetic torque in dependence on the angular rotor position. Since the voltage of the machine is not fixed with such an application, a Y- or Δ-connected stator winding is suitable with respect to its advantages as well as drawbacks.

As proposed in [2], transient voltage driven analyses with high frequency voltage pulses are additionally carried out for evaluating the suitability for a position sensorless control which relies on the position dependent inductances of the PMSM. This approach directly allows for a comparison of the numerically obtained currents with those obtained from measurements.

2. FINITE ELEMENT MODELLING

Fig. 1 shows the basic geometry with 24 poles of the investigated external rotor PMSM with an air-gap of 2 mm and an outer rotor diameter of 400 mm. In order to reduce the torque ripple of the integer slot winding, only skewed stator slots are concerned. To take into account the periodicity of the machine, the 2D finite element model consists only of two poles with repeating periodic boundary conditions at the boundaries being two pole pitches apart.

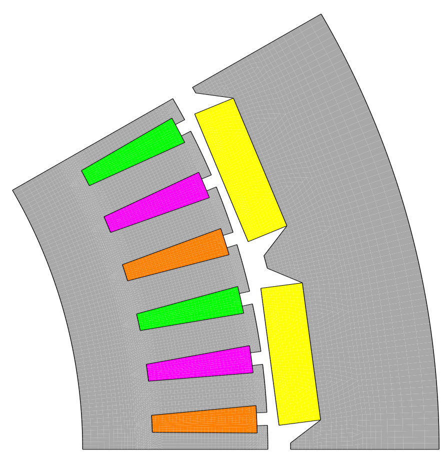

Fig. 1: Cross section of the external rotor permanent magnet synchronous machine, angular rotor position 0°

As shown in Fig. 2, all analyses utilize fully independent models of rotor and stator denoted as Ω_{rt} and Ω_{st} with an equidistant discretization in circumferential direction along the sliding surface interface Γ_{sl} within the air-gap. Both model parts are coupled by floating multipoint boundary conditions along the boundaries Γ_{rt} and Γ_{st} on the sliding surface interface Γ_{sl} in dependence on the angular rotor position [3]–[5]. This sliding surface approach completely avoids any remeshing of the air-gap regions yielding an identical quality of the numerical results for all analyses of subsequent angular rotor positions. The skewed stator slots are modelled with a multi-slice approach with a Gauss distribution of the slices [6], [7].

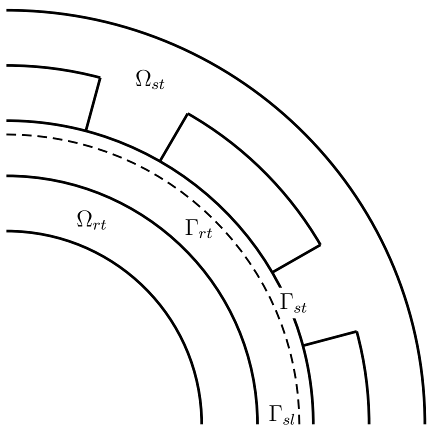

Fig. 2: Domain parts with the sliding surface approach

3. SPACE VECTOR CALCULUS

In the dq rotor fixed reference frame [8], [9], the normalized stator current and stator flux space vectors are given by

$$\underline{i}_{S,dq} = i_S\, e^{\jmath\beta} \; = i_d + \jmath\, i_q \;\; , \tag{1}$$

$$\underline{\psi}_{S,dq} = \psi_S\, e^{\jmath\vartheta} = \psi_d + \jmath\, \psi_q \;\; , \tag{2}$$

where β,ϑ are the stator current angle and the stator flux angle, respectively. The components of the stator flux linkage are usually defined by

$$\psi_d(i_d) = l_{dd}(i_d)\, i_d + \psi_M \;\; , \tag{3a}$$

$$\psi_q(i_q) = l_{qq}(i_q)\, i_q \;\; , \tag{3b}$$

where l_{dd},l_{qq} are the direct and quadrature axis inductances and ψ_M denotes the flux linkage of the permanent magnets. On the other hand, very fast changing loads require an introduction of additional cross-coupling inductances l_{dq},l_{qd} with modified flux linkages

$$\psi_d(i_d, i_q) = l_{dd}(i_d, i_q)\, i_d + l_{dq}(i_d, i_q)\, i_q + \psi_M \;\; , \tag{4a}$$

$$\psi_q(i_d, i_q) = l_{qd}(i_d, i_q)\, i_d + l_{qq}(i_d, i_q)\, i_q \;\; . \tag{4b}$$

In order to inject the stator currents in the $\alpha\beta$ stator fixed reference frame of the finite element model, the stator current and stator flux space vectors are transformed as given by

$$\underline{i}_{S,\alpha\beta} = \underline{i}_{S,dq}\, e^{\jmath\gamma} \;\; , \tag{5}$$

$$\underline{\psi}_{S,\alpha\beta} = \underline{\psi}_{S,dq}\, e^{\jmath\gamma} \;\; , \tag{6}$$

where γ denotes the electric angular rotor position.

In case of a Y-connected stator winding, any zero sequence stator currents are impossible. Therefore, the stator currents are directly deduced from

$$i_{S1} = \mathrm{Re}\big(\underline{i}_{S,\alpha\beta}\big) \;\; , \tag{7a}$$

$$i_{S2} = \mathrm{Re}\big(\underline{i}_{S,\alpha\beta}\; \mathrm{e}^{-\jmath 2\pi/3}\big) \;\; , \tag{7b}$$

$$i_{S3} = \mathrm{Re}\big(\underline{i}_{S,\alpha\beta}\; \mathrm{e}^{-\jmath 4\pi/3}\big) \;\; . \tag{7c}$$

On the other hand in case of a Δ-connected stator winding, there is an unknown zero sequence current i_0 with all phases. Therefore, the stator currents are now obtained from

$$i_{S1} = i_0 + \mathrm{Re}\big(\underline{i}_{S,\alpha\beta}\big) \;\; , \tag{8a}$$

$$i_{S2} = i_0 + \mathrm{Re}\big(\underline{i}_{S,\alpha\beta}\; \mathrm{e}^{-\jmath 2\pi/3}\big) \;\; , \tag{8b}$$

$$i_{S3} = i_0 + \mathrm{Re}\big(\underline{i}_{S,\alpha\beta}\; \mathrm{e}^{-\jmath 4\pi/3}\big) \;\; . \tag{8c}$$

The unknown zero sequence current has to be determined iteratively for each angular rotor position with all operating conditions according to the vanishing sum $u_{S1} + u_{S2} + u_{S3} = 0$ of the three phase voltages.

Neglecting the stator resistance and the cross-coupling as well as without the permanent magnets, a constant rotor angular velocity allows for the definition of a complex stator admittance which can be derived from (1)-(6) as

$$\underline{y}_S(\gamma) = \frac{\underline{i}_{S,\alpha\beta}}{\underline{u}_{S,\alpha\beta}} = \frac{1}{2\jmath\omega_S}\left(\frac{1}{l_{dd}} + \frac{1}{l_{qq}}\right) - \frac{1}{2\jmath\omega_S}\left(\frac{1}{l_{dd}} - \frac{1}{l_{qq}}\right)\frac{\underline{u}^*_{S,\alpha\beta}}{\underline{u}_{S,\alpha\beta}}\, e^{2\jmath\gamma} \;\; . \tag{9}$$

According to the two axes approximation and neglecting any saturation, this complex admittance is represented by a circle within the complex plane for any constant stator voltage $\underline{u}_{S,\alpha\beta}$. To obtain a unique information about the angular rotor position γ from the complex stator admittance (9) with all operational states, the difference $l_{dd} - l_{qq}$ of the two axes inductances should not change the sign. Thus, the magnetic saliency ratio l_{dd}/l_{qq} must be either greater or less than one under all operational conditions.

4. ANALYSIS RESULTS

4.1. Electromagnetic torque

As mentioned above, a cogging torque as small as possible is the most important criterion for a drive system of an electric vehicle. Fig. 3 and Fig. 4 as well as Fig. 5 and Fig. 6 depict load and cogging torque with various ratios b_t/τ_s of tooth width and slot pitch for both the Y- and Δ-connected stator winding. Accordingly, Table I and Table II lists the magnitudes of the significant harmonics in dependence on the ratio b_t/τ_s.

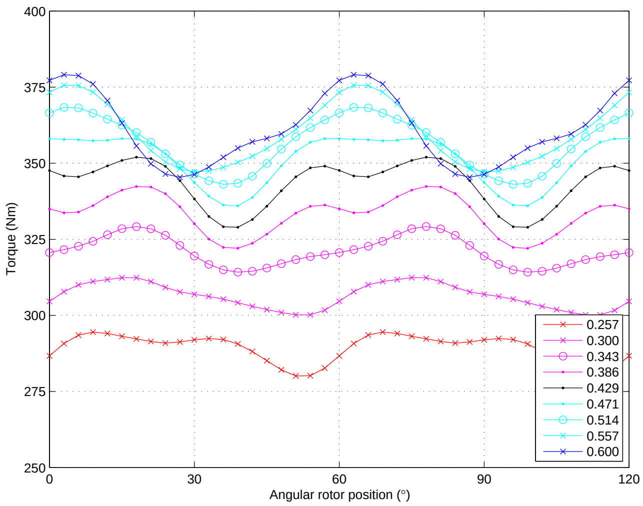

Fig. 3: Load torque with various ratios b_t/τ_s of tooth width and slot pitch, $\underline{i}_{S,dq} = \jmath$, Y-connected stator winding

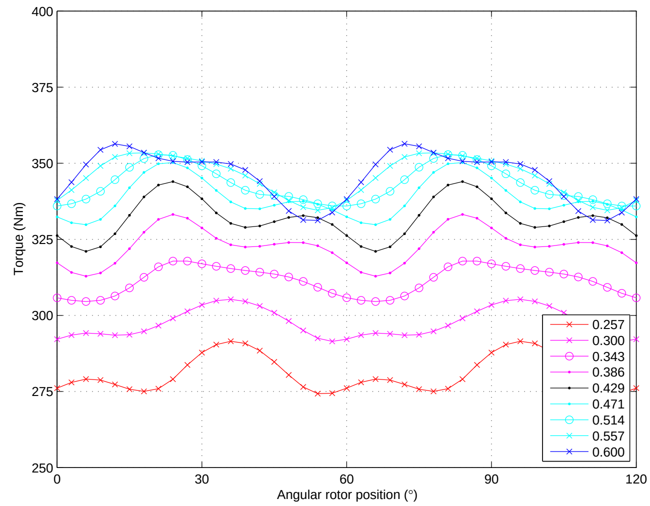

Fig. 5: Load torque with various ratios b_t/τ_s of tooth width and slot pitch, $\underline{i}_{S,dq} = \jmath$, Δ-connected stator winding

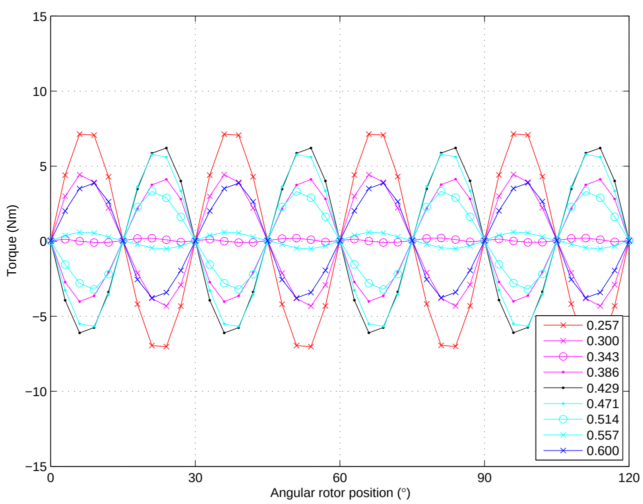

Fig. 4: Cogging torque with various ratios b_t/τ_s of tooth width and slot pitch, Y-connected stator winding

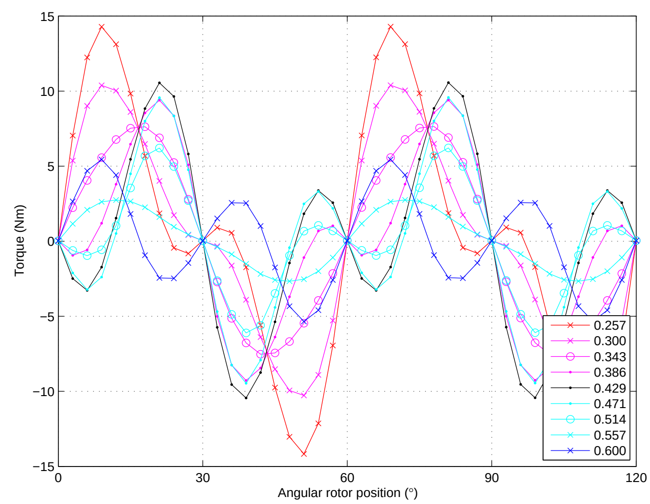

Fig. 6: Cogging torque with various ratios b_t/τ_s of tooth width and slot pitch, Δ-connected stator winding

TABLE I
LOAD AND COGGING TORQUE HARMONICS (MAGNITUDES) WITH VARIOUS RATIOS OF TOOTH WIDTH AND SLOT PITCH, Y-CONNECTED STATOR WINDING

Ratio b_t/τ_s	Average	Load Torque (Nm) 6$^{\text{th}}$ order	Load Torque (Nm) 12$^{\text{th}}$ order	Cogging Torque (Nm) 6$^{\text{th}}$ order	Cogging Torque (Nm) 12$^{\text{th}}$ order
0.257	289.2	5.3	3.7	0.0	7.4
0.300	306.4	5.6	1.5	0.0	4.3
0.343	321.1	6.4	2.3	0.0	0.1
0.386	333.3	7.5	4.9	0.0	4.1
(ID) 0.429	343.2	8.9	5.8	0.0	6.3
0.471	350.9	10.5	4.3	0.0	5.9
0.514	356.4	12.2	1.2	0.0	3.2
0.557	359.8	13.8	2.3	0.0	0.5
0.600	361.1	15.2	4.7	0.0	3.8

TABLE II
LOAD AND COGGING TORQUE HARMONICS (MAGNITUDES) WITH VARIOUS RATIOS OF TOOTH WIDTH AND SLOT PITCH, Δ-CONNECTED STATOR WINDING

Ratio b_t/τ_s	Average	Load Torque (Nm) 6$^{\text{th}}$ order	Load Torque (Nm) 12$^{\text{th}}$ order	Cogging Torque (Nm) 6$^{\text{th}}$ order	Cogging Torque (Nm) 12$^{\text{th}}$ order
0.257	280.9	6.8	4.6	9.9	6.6
0.300	297.6	6.2	2.0	8.8	3.6
0.343	311.6	6.1	1.9	7.6	0.6
0.386	322.9	6.2	5.2	6.5	4.5
(ID) 0.429	331.9	6.5	6.5	5.4	6.6
0.471	338.7	7.1	5.3	4.4	6.2
0.514	343.1	8.0	2.3	3.5	3.4
0.557	345.5	9.0	2.1	2.6	0.6
0.600	345.8	10.2	5.1	1.8	4.0

In comparison of the Y- and Δ-connected stator windings, the latter generates a lower mean value of the load torque and simultaneously a higher cogging torque with all ratios b_t/τ_s. There is a noticeable sixth harmonic in the cogging torque only for the Δ-connected stator winding which results from the zero sequence current in the three phases. Additionally, two design variations result in a significantly smaller 12^{th} harmonic in the cogging torque than the initial design. With respect to a lower saturation level, the higher value of the ratio b_t/τ_s will be preferred.

4.2. No-load voltages

Fig. 7 and Fig. 8 depict the no-load voltages of one phase with various ratios b_t/τ_s and all three phases with the initial design for the speed of 320 rpm for both the Y- and Δ-connected stator winding. Accordingly, Table III and Table IV list the magnitudes of the significant harmonics in dependence on the ratio b_t/τ_s.

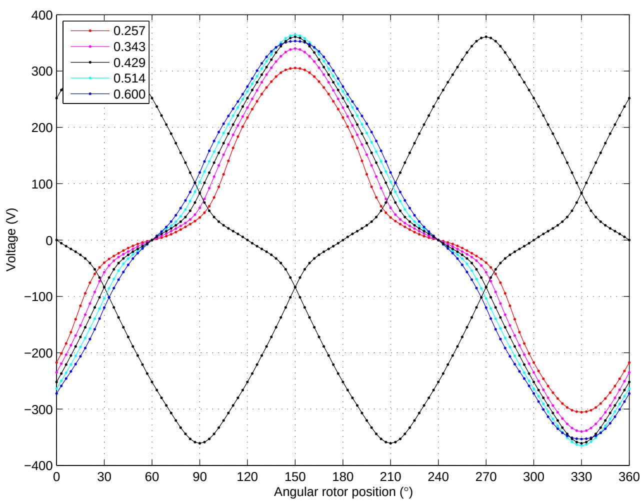

Fig. 7: No-load voltages with various ratios b_t/τ_s of tooth width and slot pitch, Y-connected stator winding

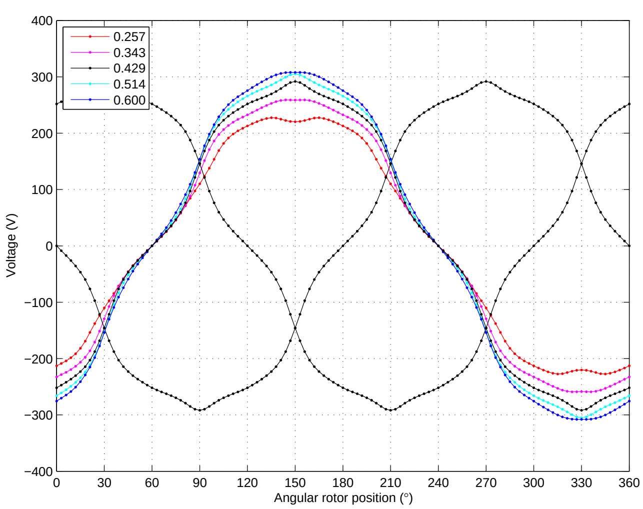

Fig. 8: No-load voltages with various ratios b_t/τ_s of tooth width and slot pitch, Δ-connected stator winding

TABLE III
NO-LOAD VOLTAGE HARMONICS (MAGNITUDES) WITH VARIOUS RATIOS OF TOOTH WIDTH AND SLOT PITCH, Y-CONNECTED STATOR WINDING

Ratio	Voltage (V)				
b_t/τ_s	1^{st} order	3^{rd} order	5^{th} order	7^{th} order	9^{th} order
0.257	239.9	73.0	4.1	6.8	3.0
0.300	255.9	71.7	4.7	2.6	4.8
0.343	270.1	69.0	4.4	1.3	4.9
0.386	282.3	65.3	3.7	4.1	4.3
(ID) 0.429	292.6	61.2	3.3	6.0	3.6
0.471	301.0	56.7	3.4	7.1	2.7
0.514	307.9	51.4	3.9	7.4	1.6
0.557	313.5	45.4	4.6	7.0	0.2
0.600	317.9	38.5	5.4	6.0	1.4

TABLE IV
NO-LOAD VOLTAGE HARMONICS (MAGNITUDES) WITH VARIOUS RATIOS OF TOOTH WIDTH AND SLOT PITCH, Δ-CONNECTED STATOR WINDING

Ratio	Voltage (V)				
b_t/τ_s	1^{st} order	3^{rd} order	5^{th} order	7^{th} order	9^{th} order
0.257	236.3	0.0	14.5	1.6	0.0
0.300	252.1	0.0	14.6	6.3	0.0
0.343	266.2	0.0	14.7	10.4	0.0
0.386	278.5	0.0	14.7	13.3	0.0
(ID) 0.429	288.8	0.0	14.7	14.5	0.0
0.471	297.4	0.0	14.7	14.4	0.0
0.514	304.5	0.0	14.9	13.4	0.0
0.557	310.4	0.0	15.0	11.9	0.0
0.600	315.3	0.0	14.8	10.0	0.0

In comparison of the Y- and Δ-connected stator windings, the latter generates a lower value of the fundamental harmonic with all ratios b_t/τ_s. Due to the high level of saturation, the no-load voltages contain a significant third harmonic with all design variations in case of the Y-connected stator winding. On the other hand, there is no third harmonic in case of the Δ-connected stator winding. Moreover, the fifth and seventh harmonics are higher with the Δ-connected stator winding than with the Y-connected stator winding.

In summary, the Y-connected stator winding, in particular due to a high third harmonic, will generate higher iron losses than the Δ-connected stator winding. On the other hand, the zero sequence current of the Δ-connected stator winding will generate slightly more power losses in the windings and more significant higher harmonics of the torque.

Finally, Fig. 9 depicts the measured no-load phase voltage for the Δ-connected stator winding with the initial design for the speed of 668 rpm. Accordingly, Fig. 10 shows the zero sequence current of both finite element analysis as well as measurements. Obviously, there is a very good agreement between simulation and measurement results.

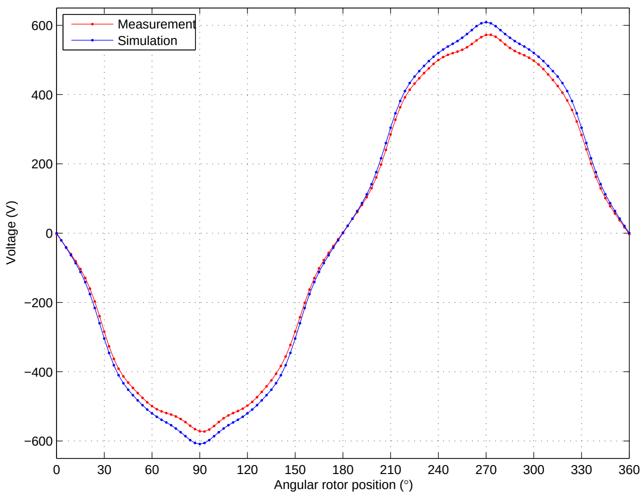

Fig. 9: No-load voltage with the initial design, Δ-connected stator winding, numerical analysis and measurement results

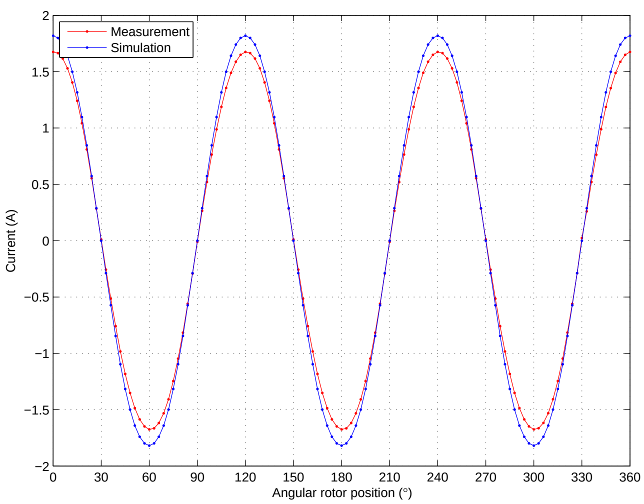

Fig. 10: No-load zero sequence current with the initial design, Δ-connected stator winding, numerical analysis and measurement results

5. CONCLUSION

The paper discusses parametric finite element analyses of a PMSM with skewed stator slots and an external rotor. In order to obtain an optimized machine design in terms of cogging torque and magnetic saliency, electromagnetic torque and no-load voltages in dependence on the angular rotor position based on geometry variations are shown in detail. As the cogging torque of the PMSM is one of the most important criterion for an application in a high performance drive system for an electric vehicle, detailed investigations concerning both Y- and Δ-connected stator winding are carried out. Consequently, an optimization of the machine design can be carried out in the design stage without a prototype of the machine.

REFERENCES

[1] Schmidt E.: "Comparison of Different Designs of Normal and Permanent Magnet Excited Reluctance Machines". *Proceedings of the 9th International Conference on Modeling and Simulation of Electrical Machines, Converters and Systems, ELECTRIMACS*, Quebec City (QC, Canada), 2008.

[2] Schmidt E., Eilenberger A.: "Calculation of Position Dependent Inductances of a Permanent Magnet Synchronous Machine with an External Rotor by using Voltage Driven Finite Element Analyses". *IEEE Transactions on Magnetics*, Vol. 45, No. 3, March 2009.

[3] De Gersem H., Mertens R., Lahaye D., Vandewalle S., Hameyer K.: "Solution Strategies for Transient, Field-Circuit Coupled Systems". *IEEE Transactions on Magnetics*, Vol. 36, No. 4, July 2000.

[4] Tsukerman I.: "Accurate Computation of Ripple Solutions on Moving Finite Element Meshes". *IEEE Transactions on Magnetics*, Vol. 31, No. 3, May 1995.

[5] De Gersem H., Weiland T.: "Harmonic Weighting Functions at the Sliding Surface Interface of a Finite Element Machine Model Incorporating Angular Displacement". *IEEE Transactions on Magnetics*, Vol. 40, No. 2, March 2004.

[6] Piriou F., Razek A.: "A Model for Coupled Magnetic-Electric Circuits in Electric Machines with Skewed Slots". *IEEE Transactions on Magnetics*, Vol. 26, No. 2, March 1990.

[7] Gyselinck J., Vandevelde L., Melkebeek J.: "Multi-Slice Finite Element Modeling of Electrical Machines with Skewed Slots – The Skew Discretization Error". *IEEE Transactions on Magnetics*, Vol. 37, No. 5, September 2001.

[8] Park R.H.: "Two-Reaction Theory of Synchronous Machines, Generalized Method of Analysis". *AIEE Transactions*, Part. I, Vol. 48, July 1929.

[9] Kovacs P.K.: *Transient Phenomena in Electrical Machines*. Elsevier, Amsterdam, 1984.

[10] Jin J.: *The Finite Element Method in Electromagnetics*. John Wiley & Sons, New York (USA), 2002.

[11] Bastos J.P.A., Sadowski N.: *Electromagnetic Modeling by Finite Element Methods*. Marcel Dekker Ltd, New York (USA), 2003.